that in the irradiance case one works with numbers; in the radiance case one works with functions and, in addition to extensive numerical details, the order of operations on functions in this case must be scrupulously observed.

Concluding Observations

One of the two main goals of this chapter has been the pair of equations (18) and (19) of Sec. 12.13. They describe the time-averaged radiance distributions $\hat{N}_+(\hat{S})$, $\hat{N}_-(\hat{S})$ directed into the aerosol and hydrosol, respectively, above and below the dynamic air-water surface. The main purpose of these equations is to form a solid mathematical and physical foundation for practical techniques of describing and predicting the average radiance distributions of wind-blown seas, lakes, and other natural hydrosols. The preceding discussion of the hierarchies of approximate theories leading from (18) and (19) of Sec. 12.13, shows that this purpose has been adequately fulfilled. Thus we were able to deduce the two classical formulas for the time-averaged apparent radiance and apparent contrasts of submerged objects as in (18) and (21). However, (18) and (19) of Sec. 12.13 allow us to go beyond these classical formulas and establish (7) and, more completely, (24) which can take into account the shielding effects of wave slopes and wave elevations from sky- and sunlight without the complications of radiometric self-interactions of the dynamic air-water surface.

The complete description of the averaged light field, with self-interactions, shieldings, and hydrosol light-fields, all in concert, as given in (18) and (19) of Sec. 12.13, has not yet been subject to numerical applications. Before this can be done, further study of the operator $R_-(X)$ in (9) of Sec. 12.13 must be made. To a first approximation we may use the $R(0,\infty)$ operators (with kernels $R(0,\infty;\xi';\xi)$) in Sec. 7.6 instead of $R_-(\hat{X})$. However, interested students after careful study will see what more can be done here.

The theory of the optical properties of the air-water surface has thus been brought to a level of completion summarized by (18) and (19) of Sec. 12.13.

12.15 Simulation of the Reflectance of the Air-Water Surface by Mechanical Devices

We conclude this chapter on optical properties of the air-water surface with descriptions of some mechanical devices which may be used to predict, with relatively little advanced mathematical computations, the average sun and sky radiance reflected from wind-blown water surfaces. The theoretical discussions throughout this chapter have demonstrated that a virtually complete theory of radiative transfer across randomly moving water surfaces can be formulated so that the reflected and transmitted radiances can, in principle, be computed in great detail. However, it is not always possible or economical to solve daily problems of applied hydrologic optics with such relatively powerful batteries of tools. In the first and main part of this section we shall round out

our theoretical studies by describing in detail a practical device which predicts the reflected radiance distribution and which is based on the theory of reflected radiance from a statistically uniform sea surface lighted by sky and sun. The motivation for such a device is the need for a simple laboratory means of predicting the apparent contrast of floating objects with respect to the background sea, as seen by observers aloft. The radiance of the sea forming the background depends, as we have seen, in part on the radiance distribution of the sky above the observed point, and the spectrum of the waves in the neighborhood of the point. Measurements of the reflected radiance distribution and spectra from aircraft are possible but occasionally inconvenient. The sea surface simulator described below was devised to permit laboratory measurements of reflected radiance distributions under widely simulated conditions of sky lighting and sea state.

The Central Idea of the Sea State Simulator

The geometric interpretation of the equation:

$$\hat{a}_\phi = \left(1 - e^{-\frac{1}{2}\frac{\tan^2\phi}{\sigma^2}}\right)$$

holds the key to the idea of the sea state simulator. As we saw in the derivation of this equation (cf. (29) of Sec. 12.5) $\hat{a}_\phi$ is the fractional horizontal area of a random sea surface over which the wave normals are tilted at angles ϕ' in the range $(0,\phi)$. If, therefore, a fixed surface of finite lateral extent could be constructed so that the normals to it obey the preceding geometric condition on $\hat{a}_\phi$ then we would have a stationary surface whose slope properties, at least statistically, are identical with those of a random moving sea surface whose mean square slope is σ^2. More genrally, it seems possible to be able to construct a surface $\hat{S}$ such that the fractional horizontal area covered by points of S at which the slope components are in the intervals $(\zeta_x \pm (1/2)\Delta\zeta_x)$, $(\zeta_y \pm (1/2)\Delta\zeta_y)$, is given by:

$$\frac{1}{2\pi\sigma_u\sigma_c} e^{-\frac{1}{2}\left[\left(\frac{\zeta_x}{\sigma_u}\right)^2 + \left(\frac{\zeta_y}{\sigma_c}\right)^2\right]}_{\Delta\zeta_x\Delta\zeta_y} .$$

The construction of $\hat{S}$ will now be described.

Ergodic Hypothesis

For the present discussion the sea surface is represented by a real-valued elevation function ζ defined on the Euclidean plane E_2 such that at each time t, and at each point (x,y) of E_2, $\zeta(x,y,t)$ is the associated elevation (now measured positive upward) of the sea surface with respect to

the datum plane E_2. The slope components of the sea surface are then represented by the functions $\zeta_x = \partial\zeta/\partial x$, $\zeta_y = \partial\zeta/\partial y$ defined on E_2 for each time t. Let G be the Heaviside function:

$$G(x) = \begin{cases} 0 & \text{if} \quad x < 0 \\ 1 & \text{if} \quad x \geq 0 \end{cases}$$

and let f be some given real-valued function on E_2. Then for each point (ξ,η) in E_2 write:

$$\text{"}Q_T(\zeta_x,\zeta_y;\xi,\eta)\text{"} \quad \text{for} \quad \frac{1}{T}\int_0^T G[f[\zeta_x(\xi,\eta,t'),\zeta_y(\xi,\eta,t')] - c]dt' \ ,$$

$$0 \leq c < \infty \quad .$$

Further, for each t and subset E of E_2, let "$|E|$" denote the area of E, and write:

$$\text{"}R_E(\zeta_x,\zeta_y;t')\text{"} \quad \text{for}$$

$$\frac{1}{|E|}\int_{(\xi',\eta')\in E} G\left[f[\zeta_x(\xi',\eta',t),\zeta_y(\xi',\eta',t)] - c\right] d\xi'\, d\eta' \quad .$$

ζ is said to be *ergodic* over $E \subset E_2$ during $[0,T]$, $T \leq \infty$, with respect to f, if for each point $(\xi,\eta) \in E$, each C, $0 \leq C < \infty$, and $t \in [0,T]$,

$$Q_T(\zeta_x,\zeta_y;\xi,\eta) = R_E(\zeta_x,\zeta_y;t) \tag{1}$$

ζ is *normally ergodic* if ζ is ergodic and

$$f(\zeta_x,\zeta_y) = \left(\frac{\zeta_x}{\sigma_u}\right)^2 + \left(\frac{\zeta_y}{\sigma_c}\right)^2 \quad , \quad \sigma_u \geq \sigma_c$$

and

$$Q_T(\zeta_x,\zeta_y;\xi,\eta) = R_E(\zeta_x,\zeta_y;t) = \int_{\{\zeta_x,\zeta_y : f(\zeta_x,\zeta_y) \geq c\}} \exp\left\{-\frac{1}{2} f(\zeta_x,\zeta_y)\right\} d\zeta_x\, d\zeta_y \quad . \tag{2}$$

We come now to the main definition of the present discussion. The graph of a function ζ forms an *ergodic cup* (cap) on a subset E of E_2 if and only if (i) E is compact, (ii) ζ is independent of t and normally ergodic on E, and (iii) ζ is continuous and concave (convex) upward on E.

The ergodic cups we shall consider will be concave (or convex) stationary surfaces of arbitrarily small lateral and vertical extent which summarize the salient statistical properties of the slopes of randomly moving irregular surfaces of large or possibly infinite lateral extent. In this discussion we will assume that the sea surface may be described by a normally ergodic function on E_2, with parameters σ_u, σ_c. The discussion will be concerned principally with the description of the parametric equations of the simplest associated ergodic cup (in principle there is an infinite variety of cups for each pair σ_u, σ_c). The simulation problem is therefore considered here only in terms of its statistical components. Thus the question of whether an ergodic cup reproduces *all* the optical properties of the original surface (i.e., those in addition to the mean square slope) is beyond the scope of the following discussion.

One may construct assemblies of ergodic cups (or caps) suitably arranged in (say) finite rectangle arrays. The array may then be placed in an environment with real or simulated lighting conditions and the resulting reflected radiance pattern photometered. To be specific in our constructions we shall discuss only ergodic cups. However, every result obtained is immediately applicable to ergodic caps.

The Discrete Case

The following problem is fundamental in the determination of an ergodic cup:

Given: - An ellipse e in E_2, of area A, with semimajor and seminor axes a and b, respectively; and a set of m positive numbers k_j, j = 1, ..., m.

Required: To find m ellipses $e_1, \ldots, e_m$ (Fig. 12.66) with the following properties:

(a) $e_j \subset e_{j+1}$, j = 1, ..., m, where $e_{m+1}=e$, such that all ellipses are concentric, and have parallel major axes.

(b) All ellipses e_j have eccentricity $[1 - (b^2/a^2)]^{1/2}$.

(c) If A_{j+1} is the area of the elliptical annulus between e_j and e_{j+1}, j = 1, ..., m then $A_{j+1}/A_j = k_j$. The solution to this problem is straightforward and is obtained as follows:

From (c):

$$A_j = k_1 k_2 \ldots k_{j-1} A_1$$

where A_1 is the area of e_1. By (a) and (c):

$$A = A_1 (1+k_1+k_1k_2+\ldots+k_1k_2\ldots k_m) \equiv A_1 K_m$$

So that:

$$A_j = A \frac{k_1 \ldots k_{j-1}}{K_m} .$$

Errata

The area of e_j is then:

$$A_1 + A_2 + \ldots + A_j = A\left[\frac{K_{j-1}}{K_m}\right]$$

which, along with (b), determines the semimajor and semimajor axes a_j, b_j, of e_j by means of equations:

$$a_j/b_j = a/b \quad ,$$

$$\pi a_j b_j = A\left[\frac{K_{j-1}}{K_m}\right]$$

Hence:

$$a_j = a\left[\frac{K_{j-1}}{K_m}\right]^{1/2} \tag{3}$$

$$b_j = b\left[\frac{K_{m-1}}{K_m}\right]^{1/2} \tag{4}$$

Clearly $a_j < a_{j+1}$, $b_j < b_{j+1}$, $j = 1, \ldots, m$, so that the remaining requirements of (a) complete the solution.

The fundamental problem solved above may be used to find a solution of the following discrete form of the ergodic cup problem which, in turn, yields the continuous solution of the main problem by an appropriate limit argument. Starting with:

$$P(\zeta_x, \zeta_y) = \frac{1}{2\pi\sigma_u\sigma_c} \exp\left\{-\frac{1}{2}\left[\left(\frac{\zeta_x}{\sigma_u}\right)^2 + \left(\frac{\zeta_y}{\sigma_c}\right)^2\right]\right\}$$

and assuming $\sigma_u \geq \sigma_c$, choose $m+2$ nonnegative numbers $C_j(n)$, $j = 0, 1, \ldots, m+1$, such that $0 \leq C_j(n) < C_{j+1}(n) \leq n$, where n is a positive integer, and such that $C_0(n) \equiv 0$, $C_{m+1}(n) = n$. Then for each positive j, the equation:

$$\left(\frac{\sigma_x}{\sigma_u}\right)^2 + \left(\frac{\zeta_y}{\sigma_c}\right)^2 = C_j^2(n), \quad j = 1, \ldots, m+1 \tag{5}$$

defines an ellipse e_j, of eccentricity $[1 - (\sigma_c/\sigma_u)^2]^{1/2}$, with center at the origin. Now, being guided by the fundamental problem, consider an ellipse of semimajor and semiminor axes $a(\sim\sigma_u C_{m+1}(n))$ and $b(\cong\sigma_c C_{m+1}(n))$, respectively. Furthermore, set:

$$k_j = \frac{\left[C_{j+1}^2(n) - C_j^2\right]\left[e^{-\frac{1}{2}C_{j+1}^2(n)} + e^{-\frac{1}{2}C_j^2(n)}\right]}{\left[C_j^2(n) - C_{j-1}\right]\left[e^{-\frac{1}{2}C_j^2(n)} + e^{-\frac{1}{2}C_{j-1}^2(n)}\right]}, \quad j = 1, \ldots, m.$$

These m numbers and the given ellipse define a fundamental problem of the kind solved above. The solution of the problem yields a set of m ellipses, which in turn define m elliptical annuli. These m annular regions along with e_1, comprise the domain of a continuous function ζ whose graph over each annulus is an elliptical conical surface on which the slope components (ζ_x, ζ_y) are to satisfy the equation (5). The section of this surface by the xz plane (cf., Fig. 12.67) is a

Fig. 12.66

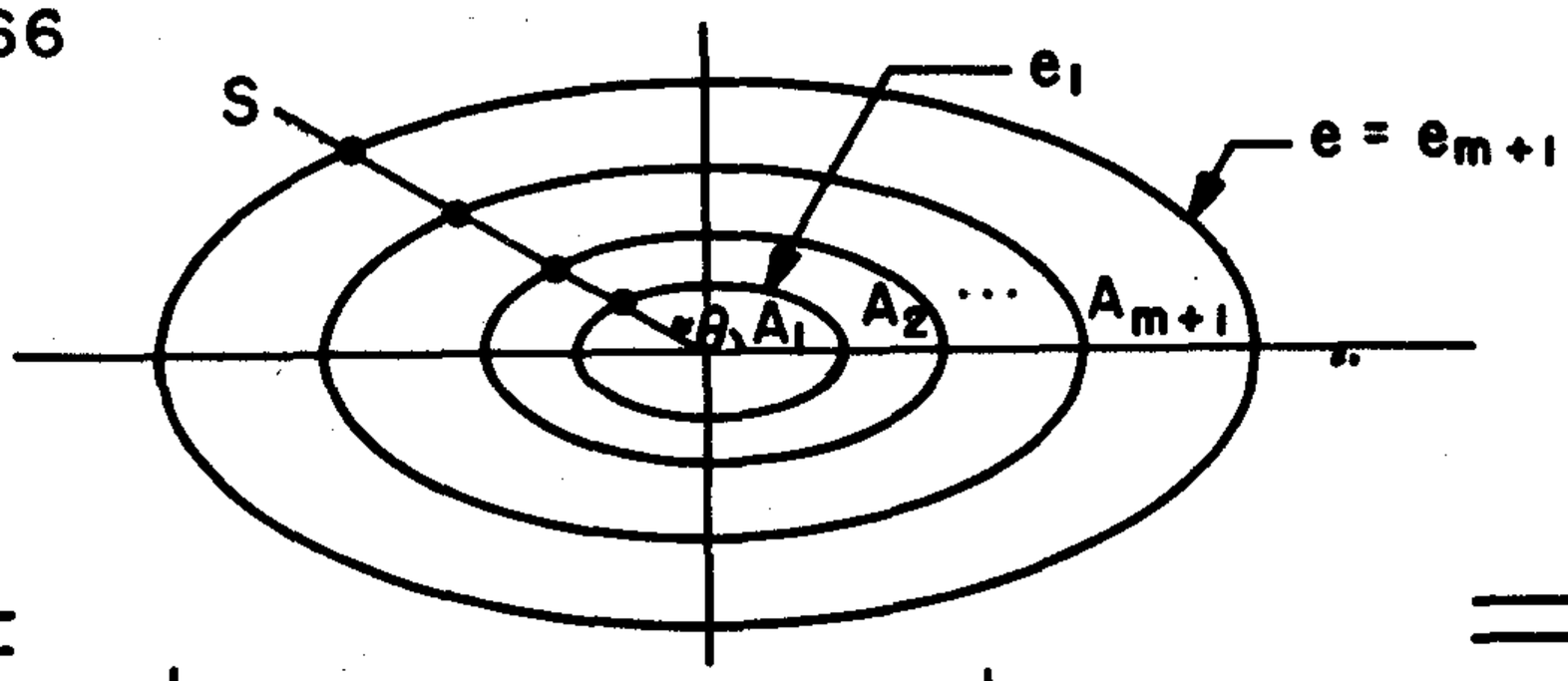

Fig. 12.67

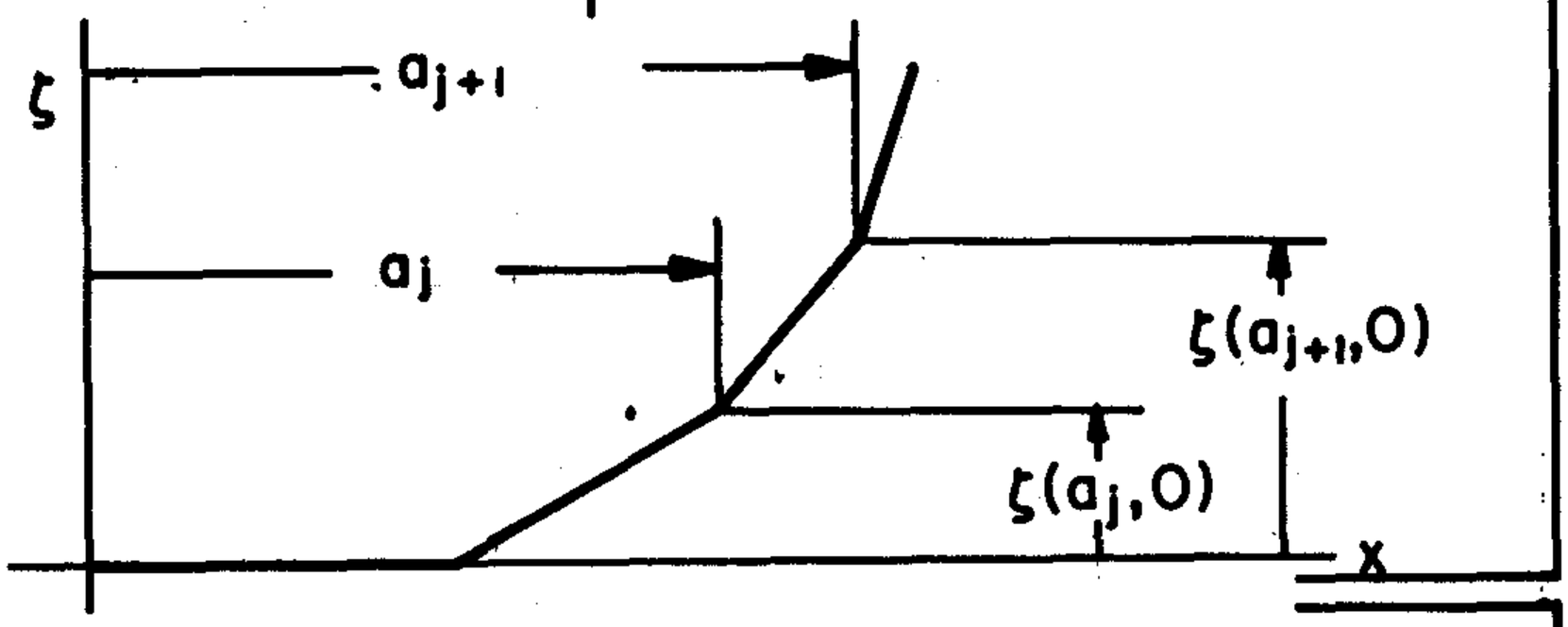

Fig. 12.68

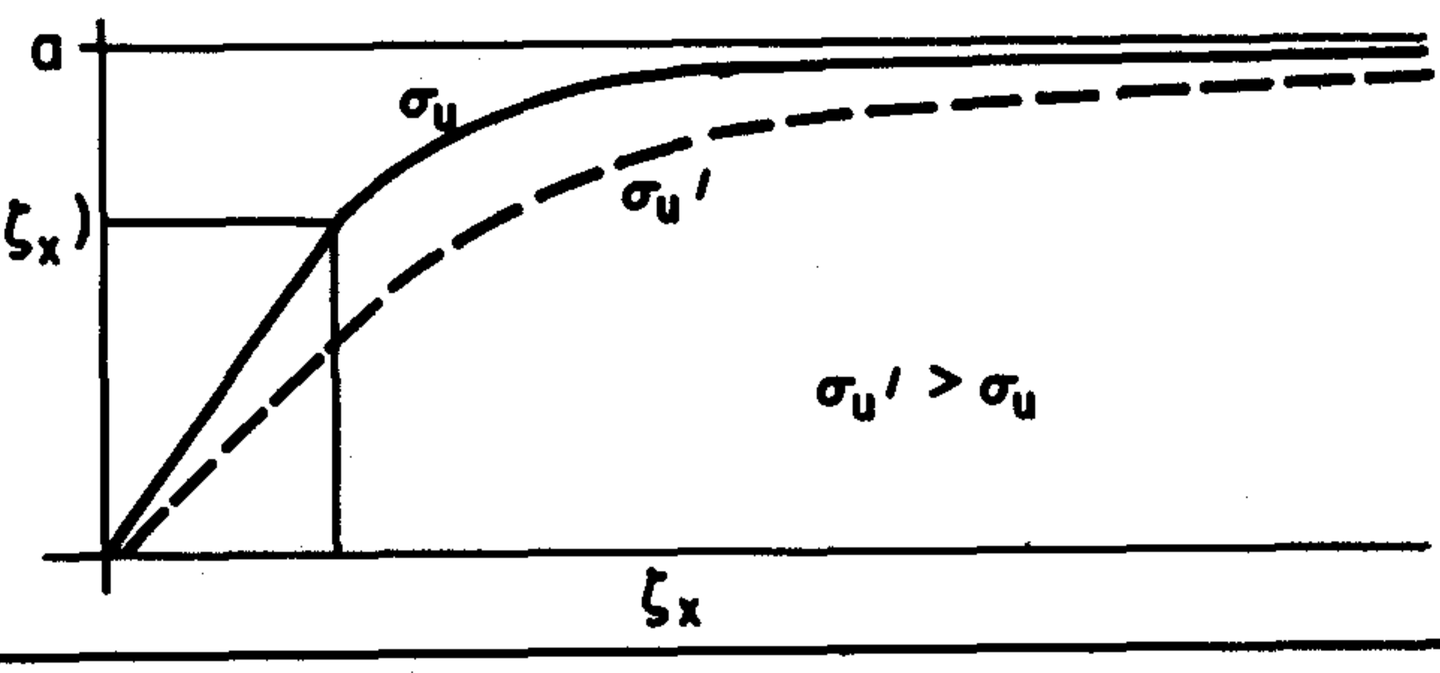

FIG. 12.66-12.68 Construction details for the ergodic-cup, sea-surface simulator.

curve composed of m+1 straight line segments whose equations are:

$$\frac{\zeta(a_{j+1},0) - \zeta(a_j,0)}{a_{j+1} - a_j} = \zeta_x(a_{j+1}) = \sigma_u C_{j+1}(n), \quad n = 1, \ldots, m$$

with:

$$\zeta_x(a_1) = 0$$

$$\zeta(a_1,0) = 0 \quad .$$

By conditions (a), (b) of the fundamental problem, this profile in principle determines the entire surface. The surface clearly satisfies a discrete version of the definition of an

ergodic cup, namely the intuitive area definition in the introduction above, or its formal counterpart (2).

In order to construct the ergodic cup in detail, some explicit analytical formulas may be derived for the slope of the surface along a slice S-S by a plane set at an arbitrary angle θ from the x-axis (cf. Fig. 12.66). It is easy to see (cf. (97) of Sec. 12.4 with $m_{11} = 0$) that the slope $\zeta_\theta(r_{j+1})$ of the surface in the slice S-S and over e_{j+1} is given by:

$$\zeta_\theta(r_{j+1}) = C_{j+1}(n)\,[\sigma_u^2 \cos^2\theta + \sigma_c^2 \sin^2\theta]^{1/2}$$

and that the corresponding segmental equations are:

$$\frac{\zeta(r_{j+1},\theta) - \zeta(r_j,\theta)}{r_{j+1} - r_j} = \zeta_\theta(r_{j+1}) \quad , \quad j = 1, \ldots, m \quad .$$

with:

$$\zeta_\theta(r_1) = 0$$

$$\zeta(r_1,0) = 0$$

for every θ, $0 \leq \theta \leq 2\pi$.

In the event that $\sigma_u = \sigma_c$, we have $\zeta_\theta(r_{j+1}) = \zeta_x(a_{j+1})$ for every θ, $0 \leq \theta \leq 2\pi$, and the ergodic cup is a surface of revolution. The number r_j is the radial distance from the origin to e_j.

The Continuous Case

From (3), into which the present forms of the k_j have been introduced, we have

$$\frac{a_j}{a} = \left[\frac{K_{j-1}(n)}{K_m(n)}\right]^{1/2} = \left[\frac{\sum_{i=o}^{j}\left[C_{i+1}^2 - C_i^2\right]\left[e^{-\frac{1}{2}C_{i+1}^2} + e^{-\frac{1}{2}C_i^2}\right]}{\sum_{i=o}^{m}\left[C_{i+1}^2 - C_i^2\right]\left[e^{-\frac{1}{2}C_{i+1}^2} + e^{-\frac{1}{2}C_i^2}\right]}\right]^{1/2}$$

where for brevity we have written "C_j^2" for $C_j^2(n)$. A similar formula holds for b_j/b. A transition to the continuous case now can be made by the usual method of going from a discrete approximation of the Riemann integral, to the integral itself. The differences $C_{i+1}^2 - C_i^2$ may be written as $(C_{i+1}+C_1)(C_{i+1}-C_i)$, so that $(C_{i+1}-C_i)$ acts like an element of length along the integration domain. By holding n fixed, and letting $m \to \infty$, so that the largest of the differences $C_{i+1}-C_i$ goes to zero, we see that the denominator $K_m(n)$ in a_j/a has the limit:

$$\lim_{m\to\infty} K_m(n) \equiv K(n) = 4\int_0^n t\, e^{-\frac{1}{t}t^2}\, dt$$

$$= 4\left(1 - e^{-n^2/2}\right) \quad \ldots$$

Further, as we let $m \to \infty$, also let j vary (as an integer) in such a way that $C_j \to \psi (= (\zeta_x/\sigma_u)$, or $(\zeta_y/\sigma_c))$ where ψ is a fixed real number in [0,n] and independent of n. Associated with the limit of C_j is that of a_j, which we shall denote by "$a(\zeta_x)$".

Next observe that

$$\lim_{m\to\infty} K_{j-1}(n) \equiv K(\psi,n) = 4\int_0^{\psi} t\, e^{-\frac{1}{2}t^2}\, dt$$

$$= 4\left(1 - e^{-\frac{1}{2}\psi^2}\right).$$

Then letting $n \to \infty$, we have

$$\lim_{n\to\infty} K(n) = 4$$

and

$$\lim_{n\to\infty} K(\psi,n) = 4\left(1 - e^{-\frac{1}{2}\psi^2}\right) \quad .$$

Hence

$$\frac{a(\zeta_x)}{a} = \left[1 - e^{-\frac{1}{2}\left(\frac{\zeta_x}{\sigma_u}\right)^2}\right]^{1/2}, \quad 0 \le a(\zeta_x) \le a \qquad (6)$$

$$\frac{b(\zeta_y)}{b} = \left[1 - e^{-\frac{1}{2}\left(\frac{\zeta_y}{\sigma_c}\right)^2}\right]^{1/2}, \quad 0 \le b(\zeta_y) \le b \quad . \qquad (7)$$

Equations (6) and (7) define the functions $a(\zeta_x)$ and $b(\zeta_y)$ of the variables ζ_x and ζ_y, respectively, having given σ_u and σ_c as fixed parameters. Conversely, with σ_u, σ_c fixed, (6) and (7) define ζ_x, ζ_y as functions of $a(\zeta_x)$ and $b(\zeta_y)$. (See Figure 12.68 which schematically depicts the case for $a(\zeta_x)$. The figure is not drawn to any particular scale.)

It follows that

$$\zeta(x,0) = \int_o^x \zeta_x(t)dt \quad , \quad 0 \leq x \leq a \tag{8}$$

defines the xz section of a surface which is readily verified to be an ergodic cup for each choice of a. The analysis of the discrete case shows that the above xz section is sufficient in principle to determine the entire ergodic cup. For detailed constructions, the continuous version of $\zeta(r_{j+1})$ is readily derived. If $\sigma_u = \sigma_c$, the ergodic cup is a surface of revolution.

In our opening discussion of this section, wherein the central idea of the sea state simulator was outlined, reference was made to the analytic form of the fractional area a of a given region of sea surface which was tilted at an angle ϕ from the horizontal. We are now in a position to see that opening remark in its proper perspective, with the help of (6) and (7). Multiplying the corresponding sides of these equations together we find

$$\frac{a(\zeta_x)b(\zeta_y)}{ab} = \left(1 - e^{-\frac{1}{2}\left(\frac{\zeta_x}{\sigma_u}\right)^2}\right)^{1/2} \left(1 - e^{-\frac{1}{2}\left(\frac{\zeta_y}{\sigma_c}\right)^2}\right)^{1/2}$$

Now, for a given ψ which defines an elliptical contour as in (5), we have $\psi = (\zeta_x/\sigma_u) = (\zeta_y/\sigma_c)$, and we can write the preceding equations as:

$$\frac{A_\psi}{A} = \left(1 - e^{-\frac{1}{2}\psi^2}\right)$$

where $A_\psi = \pi a(\zeta_x)b(\zeta_y)$, and $A = \pi ab$. A_ψ is the projected area of the ergodic cup on a horizontal surface for points where the surface normal slope is less than or equal to ψ. Writing "ϕ" for arctan ψ, and "$\hat{a}_\phi$" for A_ψ/A, we obtain the ergodic cup version of (29) of Sec. 12.5.

Some General Observations on the Ergodic Cup Device

Figure 12.68 and equation (8) indicate that the depth of a cup increases with increasing sea state, thus simulating the observed increase of mean elevation of real waves with sea state. Hence the shielding of smaller slopes by larger slopes on reacl waves is reproduced--at least qualitatively and in the same direction--by an ergodic cup. Generally speaking, the curvature of a cup in the small-slope regions increases with increasing sea state. (For spectral estimates of curvature, see (24) of Sec. 12.8.) Further,

the curvature of a cup in the large-slope regions remains relatively constant with changing sea state. In short, the overall curvature of an ergodic cup varies directly with the sea state parameters in such a way as to qualitatively reproduce the observed overall change of curvatures of real waves with changing sea state. It is not to be expected, however, that these depth and curvature features of an ergodic cup *quantitatively* represent the mean depths and mean curvatures in wave patterns which are to be found on a real sea.

Sea Simulator Devices Beyond the Ergodic Cup

The concept of an ergodic cup as developed here is limited principally to the simulation of the *slope* properties of random sea surfaces. In view of the increasing numbers of optical properties of the sea surface required beyond slope properties (in particular mean height data are required) in order to make further progress in hydrologic optics, it is clear that further research is needed in the art of simulating the dynamic air-water surface by means of mechanical, electrical or optical devices.

A possible area of research in optical sea state simulation would be with laboratory (rather than natural) hydrosols on the surface of which is induced, by acoustic (or possibly mechanical) means, standing (or progressive) wave patterns with realistic directional spectra $E(\mathbf{k})$. A perusal of the linearized equations for surface waves shows that this is in principle quite feasible. By careful control of the induced wave patterns it may be possible to superimpose one standing wave pattern on another until a given $E(\mathbf{k})$ is closely approximated by that of the dynamic test surface. In the initial stages of the study, the patterns should be analyzed harmonically to see the range of directional spectra possible over the test-controlled hydrosol. It may be possible to reproduce Neumann (or other gamma type) spectra with the standing wave patterns and obtain correct scale relations with respect to natural capillary and gravity wave spectra. Once sufficient techniques have been learned, the test-controlled hydrosol could perhaps be "tuned" to a given spectrum, and photometered under a prescribed radiance distribution, to obtain the requisite reflectance properties of its real counterpart. The advantages of such a tuned laboratory hydrosol are obvious: real water could be used in such a way that Fresnel reflectance properties would be realistically reproduced; furthermore, wave slope and wave height characteristics, if properly scaled, could simulate both slope and height shielding effects of natural waves.

<< Table of Contents << Title Page >> Next Page >>

12.16 Bibliographic Notes for Chapter 12

The Fresnel laws of reflection and refraction given in Sec. 12.1 may be found in any standard text on optics. However, the general connection between the electromagnetic field and the radiance distribution from which (7) of Sec. 12.1 is derived appears to be relatively new, and may be found in Sec. 124 of [251]. The results of exact reflectance calculations for cardioidal radiance distributions as presented in Example 2, were first given in [215].